



## Tailoring methodologies for the architecture of organometallic frameworks of Bi(V) derived from antibiotics: Spectral, MS, XRPD and molecular modeling with antifungal effectiveness

Rajni Johar,<sup>a\*</sup> Rajiv Kumar,<sup>b</sup> and Anil Kirshan Aggarwal<sup>b</sup>

<sup>a</sup>Department of Chemistry, G.G.S. I.P. University, New Delhi, 110002, India

<sup>b</sup>Department of Chemistry, SC, University of Delhi, New Delhi 110027, India

Received 05-05-13 Accepted 26-05-13

### ABSTRACT

This communication describes formulation and designing methodology to discover architectural features of organometallic frameworks (OMFs) derived from the mixer of antibiotics drugs [L1 and L2] and Bi(V). Ligand (L1) was the mixer of two antibiotic drugs i.e. 5-(2,4-diguanidino-3,5,6-trihydroxy-cyclohexoxy)-4-[4,5-dihydroxy-6(hydroxymethyl)-3-methylamin-tetrahydropyran-2-yl]oxy-3-hydroxy-2-methyltetrahydrofuran-3-carbaldehyde and 2-(amino-hydroxymethylidene)-4-dimethylamino-6,10,11,12-tetrahydroxy-6-methyl-4,4a,5,5a-tetrahydro-tetracene-1,3,12-trione. Another ligand, (L2), was the mixture of two antibiotic drugs (6R)-6-( $\alpha$ -phenyl-D-glycylamino) penicillanic acid and its hydroxyl derivative. Effective encapsulation between ligands and metal ion was highly dependable on fragmentation constraints of ligands and reactivity of Bi(V). The formation of OMFs was verified by various physicochemical and spectroscopical investigations i.e. elemental analysis, electronic, IR, <sup>1</sup>H-NMR, <sup>13</sup>C-NMR, mass spectroscopy, molecular modeling and XRPD patterns analysis. OMFs were highly capable to achieve pharmacophore geometries. Stability of OMFs was differed because of the variation of architectural features of concerned ligands which were not readily and rapidly tailored and achieved by any means. OMFs were screened extensively in-vitro against a number of pathogens i.e. *Candida albicans*, *Aspergillus flavis* and *Candida glaberata* which were responsible for various diseases. Results obtained revealed that OMFs have comparatively much higher antifungal activity than ligands.

**Keywords:** Organic metal frameworks (OMFs); Antibiotic drugs; Bismuth(V); Pharmacophore geometry; Antifungal Activity

### INTRODUCTION

Bismuth is a unique element in terms of its low level of toxicity and non-carcinogenic nature, despite its heavy metal status. Traditionally, inorganic bismuth compounds have found widespread uses in medicine and veterinary practice. Various types of bismuth salts have been introduced as fungicides.<sup>1</sup> Bismuth containing pharmaceuticals are most commonly used in the eradicate *Helicobacter pylori*, a Gram-negative bacterium that causes peptic ulcers, gastric cancer and other diseases of the gastrointestinal tract<sup>2</sup> due to their astringent, bacteriostatic, and disinfectant actions.

However, bismuth salts exhibit only modest antibacterial activity. Compounds of bismuth(V) do not exist in solution.<sup>3</sup> Major applications of bismuth compounds include use in pharmaceuticals, ceramics, modern electronic components, cosmetics, plastics, pigments, paints and paint dryers, semiconductors, alloys and as a carrier for U-235 or U-233 fuel in nuclear reactors. Pharmaceutical uses of bismuth containing metallodrugs have expanded to peptic ulcer treatments and topical dermatological creams.

Methodology for the formulation of such systems from the mixer of antibiotics and Bi(V) was designed and tailored. After effective encapsulation of derived ligands with Bi(V), Organometallic frameworks (OMFs) were formed.<sup>4</sup> During the formulation of OMFs, new bonds came into existence according to binding capabilities of donor atoms of ligands towards Bi(V). Scientific validation of such magical coordination was verified by physical and analytical analysis as well as spectroscopic techniques. The enormous potentials of such OMFs have a key role in the discovery of newer metallodrugs with novel mechanism of action.<sup>5</sup> It has been suggested that enzyme inhibition played an important role in the antimicrobial activity of bismuth.<sup>6,7,8</sup> This article updates relevant advances in the past few years, concerning the application of bismuth in innovative synthetic processes

### Address:

Corresponding Author: Dr. Rajni Johar  
Department of Chemistry, G.G.S. I.P. University, New  
Delhi 110002, India  
Email: chemistry\_rajiv@hotmail.com

----

Cite as: *J. Integr. Sci. Technol.*, 2013, 1(1), 54-64.

© IS Publications JIST ISSN 2321-4635

for the preparation of Bi-OMF having medicinal interest. Biological evaluation and potential medicinal applications of Bi-OMFs were discussed and judged. Additionally OMFs were tested against fungal strain i.e. *Candida albicans*, *Aspergillus flavus* and *Candida glabrata*. Results obtained were reported and presented graphically.

## RESULTS AND DISCUSSION

Elemental analysis (CHN) was in good agreement with the molecular formulation of OMFs. Reported OMFs may possess the general composition  $[M(L)]$  and  $[M(L)]X_3$  [where L = Ligand L and X =  $OCIO_3^-$ ]. On the basis of CHN data, their molecular formula may be assigned. Results obtained were presented in table 1. The molar conductance measurement of OMFs in DMSO corresponds to non-electrolytic nature.

**Table 1.** Elemental analysis (%) of OMFs

OMFs	Empirical Formula	Elemental analysis: Found/calculated (%)				
		C	H	N	S	Bi
OMF-1	$C_{44}H_{61}BiN_8O_{20}$	42.51 (42.93)	4.75 (4.99)	9.02 (9.10)	-	16.91 (16.98)
OMF-2	$C_{32}H_{36}BiC_{13}N_6O_{21}S_2$	31.41 (31.50)	2.90 (2.97)	6.71 (6.89)	(5.12) (5.26)	17.02 (17.13)

## IR Spectra

The characteristic assignments of IR frequencies derived from the IR spectra of OMFs were discussed. After the comparison between IR spectra of OMFs and free ligands, remarkable differences were made, table 2. Certain vibrational bands in the IR spectra of free ligands and OMFs were very useful to determine the mode of bonding between functional groups ( $>C=O$  and  $-NH-$ ) and Bi(V). The absorption at  $778-770\text{ cm}^{-1}$  and  $1422-1116\text{ cm}^{-1}$  observed were due to the presence of phenyl moieties in ligands and OMFs.<sup>9</sup> In addition, there were fascination bands at  $1587-1576\text{ cm}^{-1}$  and  $1417-1411\text{ cm}^{-1}$  confirmed the presence of five member rings in ligands and OMFs. The broad bands were observed at  $3452-3350\text{ cm}^{-1}$  in the spectra of free ligands showed the presence of free hydroxyl groups  $\nu(OH)$ , which were slightly differed in OMFs suggesting the coordination of phenolic oxygen ( $-OH$ ) may or may not be takes place through deprotonation of this group during the

formation of OMFs. The appearance of new bands at  $1300-1297\text{ cm}^{-1}$  corresponding to  $\nu(-C-O-)$  indicating the formation of new bonds between oxygen and Bi(V) after deprotonation of some PhOH.<sup>10</sup> Further, I.R. spectra of ligand and OMFs showed the presence OH groups and their related peaks were observed at  $3237-3316\text{ cm}^{-1}$  which was closed to earlier findings that some PhOH groups were not participated in the bond formation Bi-O.

A group of sharp and intense bands corresponding to primary and secondary amine ( $-NH_2$  or  $-NH-$ ) groups were detected at  $3370-3360$  to  $3312-3302\text{ cm}^{-1}$ . Another distinguish peaks were observed at  $1628-1616\text{ cm}^{-1}$  which confirmed the presence of free carbonyl ( $>C=O$ ) groups. IR spectra of mixed ligands showed strong medium intensity bands at  $536-535\text{ cm}^{-1}$  confirming the presence of  $\nu(C-O)$  vibrations.<sup>11</sup> IR spectra of OMFs showed characteristic

change i.e. blue shift, which confirmed the bonding between used metal and the donor atoms of the ligand, especially observed for secondary amino groups. The bonds formation between Bi(V) and O/N showed characteristics features of OMFs as reported earlier.<sup>12</sup>

In the spectra of mixed ligands, sharp bands were observed at  $2745-2640\text{ cm}^{-1}$  could be assigned to carboxylic groups  $\nu(COOH)$  and remained unaffected during chelation. The carbonyl ( $>C=O$ ) group of indole ring appeared at  $1725-1734\text{ cm}^{-1}$  in ligands but these bands disappeared in the IR spectrum of OMC-2. Appearance of new bands at  $\sim 1705\text{ cm}^{-1}$  in the IR spectra of OMF-2 showing thereby the involvement of carbonyl ( $>C=O$ ) groups of indole ring confirmed the formation of framework. It is further confirmed by the appearance of sharp band at  $520-535\text{ cm}^{-1}$  assignable to (Bi-O) stretching vibrations. This clearly indicates the carbonyl group of ligand ( $L^2$ ) participated in framework formation. Furthermore, the

**Table 2.** Assignments of relevant IR frequencies of OMFs

OMFs	$\nu(OH)$	$\nu(>N-H)$	$\nu(Ph-O-)$	$\nu(COOH)$	$\nu(-C-O-)$	$\nu(Bi-N)$	$\nu(M-O)$	$\nu(OCIO_3)$
OMF-1	3452, 3390, 3327	3270, 1312	1750, 1050	2745	1300	-	445, 440, 420	-
OMF-2	3410, 3350, 3326	3260, 1302	1750, 1050	2640	1297	612	442, 421, 416	1181, 1112, 650, 610

separation between these vibrations was nearly  $15\text{ cm}^{-1}$ , indicating the new bonds formation (Bi-O). Bridging/chelation can therefore be excluded, and it must be assumed that carbonyl ( $>\text{C}=\text{O}$ ) formed bonds with Bi(V). Moreover, values observed in OMFs below  $450\text{ cm}^{-1}$  would be expected for bridging or chelating carbonyl groups.<sup>13</sup> The comparison of the IR spectra of the ligands with their OMF-2 principally revealed that carbonyl group bonded to Bi(V). In addition to this band at  $1685\text{--}1695\text{ cm}^{-1}$  attributed to  $\nu(\text{C}-\text{O})$  stretching in the ligands indicating the involvement of oxygen of carbonyl groups. Further conclusive evidence of the coordination of the ligand with Bi(V) was established by the far-IR spectra in which new bands in the range of  $445\text{--}416\text{ cm}^{-1}$  assigned to Bi-O<sup>14,15</sup> were observed. IR spectrum of Bi-OMCs also exhibited an intense band approximately between  $1181$  and  $1112\text{ cm}^{-1}$  along with a weak band at between  $650$  and  $610\text{ cm}^{-1}$ . This is due to the presence of perchloate ( $\text{OClO}_3$ ) in the primary coordination sphere of OMCs.

### UV Spectra

Electronic spectra of OMFs of Bi(V) showed transitions at  $360\text{--}230\text{ nm}$ , figure 1. A shoulder band was observed at  $245\text{ nm}$  in the spectrum of ligand assigned to  $n \rightarrow \pi^*$  transition within  $-\text{OH}$  group of hydroxyl moiety. A little deviation observed in OMFs for these transitions appeared for  $-\text{OH}$  comparatively to the spectrum of free ligand. It revealed that the involvement of  $-\text{OH}$  groups in chelation due to deprotonation, confirmed the formation of  $(-\text{O}-\text{Bi}-)$  bond. Owing to this, new transitions were observed at  $325\text{--}275\text{ nm}$  assigned to  $-\text{O}-\text{Bi(V)}$  as ligand-to-metal charge transfer (LMCT) transition. The spectra was featureless in the visible region, for  $d^{10}$  Bi(V) ion; however, OMFs showed some intense absorptions in UV, readily assignable to  $-\text{O}-\text{Bi(V)}$  as LMCT. The intensity of Bi-O- absorption at  $240\text{ nm}$  to be roughly consistent with new bond formation (Bi-O-) because of charge transfer and the high-energy band at  $278\text{ nm}$  was assigned to a charge-transfer, metal  $\rightarrow$  ligand or vice versa.

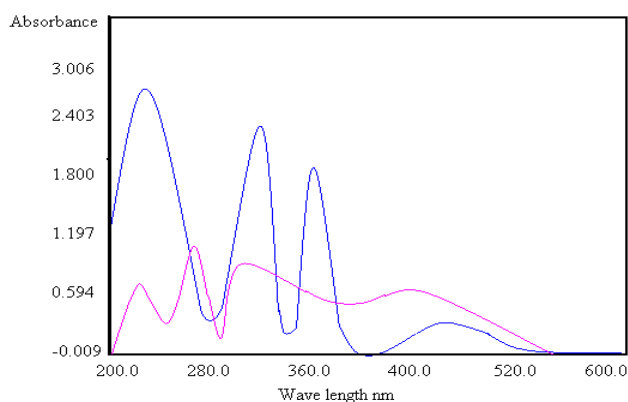


**Figure 1.** Electronic spectra of OMF-1 (blue) and OMF-2 (pink).

### $^1\text{H}$ -NMR Spectra

$^1\text{H}$  NMR spectra of ligands and OMFs in  $\text{CDCl}_3$  were compared to authenticate the chelation, the main differences were observed for the peaks of hydroxyl, carbonyl and secondary amine groups. The conclusions drawn from the

$^1\text{H}$ -NMR spectral studies led further support for the formation of bonding.  $^1\text{H}$  NMR spectral data of L-1 showed single resonance at  $11.20\text{--}12.50\text{ ppm}$ , which was absent in the spectra of OMF-2, indicating the replacement of the hydroxyl protons by Bi(V). For instance,  $^1\text{H}$  NMR spectrum of OMF-2 showed the presence of signals between  $13.00\text{--}10.00\text{ ppm}$  due to presence of hydroxyl ( $\text{OH}$ ) protons of the ligand confirmed un-coordinated behaviour of this group during the formation.<sup>16</sup> The OMFs showed a frameworks pattern at  $8.15\text{--}6.90\text{ ppm}$  for aromatic protons, and some peaks at  $7.95\text{--}7.10\text{ ppm}$  showed the presence of saturated ring system in the ligand moieties.<sup>17</sup> The appearance of signals due to  $-\text{NH}-$  protons in the ligand and absence of these peaks at the same positions in the spectra of OMF-1 showed involvement of this group in coordination. This shifting also supported the bond formation through nitrogen atom.  $^1\text{H}$  NMR spectra of OMFs and ligands ( $\text{L}^1$  or  $\text{L}^2$ ) gave signal corresponding to  $(-\text{NH}_2)$  primary amine at  $6.8\text{ ppm}$  and carboxylic protons at  $9.2\text{ ppm}$  which confirmed there was no interaction of these groups with Bi(V).

### $^{13}\text{C}$ NMR Spectra

The  $^{13}\text{C}$ -NMR spectral data along with assignment of characteristic signals of ligands and OMFs were discussed. The signals due to carbon atoms attached to  $>\text{C}=\text{O}$  and  $-\text{NH}-$  groups in OMFs appeared at  $176.0$  to  $178.6\text{ ppm}$  respectively. However, in the spectra of the corresponding OMFs, these peaks appeared at  $180.8\text{--}186.2\text{ ppm}$  ( $>\text{C}=\text{O}$ ) and at  $150.1\text{--}152.5\text{ ppm}$  ( $\text{C}-\text{N}-\text{Bi}$ ), respectively. The considerable shifts in the positions of these signals clearly indicate the involvement of these functional groups in bond formation with Bi(V). The occurrence of resonances at  $118.2$  and  $150.6\text{ ppm}$  were defined as aromatic carbon signals.<sup>18</sup> Although it is also possible that shifting of  $(=\text{N}-\text{C})$  carbon signal and  $(>\text{C}=\text{O})$  carbon signal was because of a change in hybridization of nitrogen and oxygen attached to Bi(V). In the light of IR, UV, and  $^1\text{H}$  NMR spectral studies it seems more plausible that the shifting in these carbons peaks was due to the involvement of oxygen of  $>\text{C}=\text{O}$  and nitrogen of  $>\text{N}-\text{C}$  in bonding.

### TOF-MS Spectra

The benefits of mass spectrometry in the study of supramolecular chemistry were as follows: investigation of molecules and complexes in the gas phase allows determination of the intrinsic properties without interference from solvent or counter ion. TOF-MS spectra of OMFs showed molecular ion species  $[\text{M}]^+$  and various other peaks corresponding to the fragmentation of degraded species. The patterns of peaks gave clear impression of the successive degradation of the target compound with the series of peaks corresponding to the various fragments with different intensities. The intensity detected for particular peak was directly related to the stability of degraded fragments. Molecular ion peaks corresponding to the fragments (ligand or fragments of the ligand with metal or metal + ligand) were observed to confirm their molecular formula.<sup>19</sup>

In initial peaks of OMFs were degraded into various fragments. Molecular ion peaks of OMFs were present at  $1229/1271$  ( $m/z$  values) with high intensity. Due to

degradation, another fragment patterns for OMF-1 and OMF-2 were appeared at 1516/1231/789/540 and 1710/1661/1430/1210 with different intensity respectively. Strong peaks were for OMF-1 and OMF-2 were observed at 810/650/431 and 1112/980/711/510 with different intensity separately.

In the TOF-mass spectra of OMF-2 and OMF-1, initial fragmentation patterns were found similar to the ligand and also showed an additional peak indicating the mass loss. Mass degradations patterns provide most important information about the fragmentations isotropic ratio corresponding to Bi(V) with the ligand fragments. On the basis of above discussion, a mononuclear nature of OMFs has been proved and may be assigned as  $[M+(\text{fragments of the ligand})]$ . In the mass spectra of OMF-1 and OMF-2, molecular ion peaks (ligand + metal) were represented the final molecular ion peak ( $m/z$ ) for the reported compounds. The molecular ion peaks for OMFs were detected due to loss of the ligand moiety. Successive fragmentation was observed by the loss of different groups (Me, Bu, Ph) until the Bi<sup>+</sup> ion was obtained. In the alternative route attached groups are eliminated first and in the next step a molecule of CO<sub>2</sub> is evolved from the ligand moiety. In the successive steps the remaining substituents are lost from the bismuth atom.

#### XRPD Analysis

XRPD spectra were observed and interconnected graphs of OMFs gave straightforwardly substantiate alignments in sequence about purity of OMFs. All the data related to this learning was calculated and specified in table 3. The indexing procedures performed using (CCP<sub>4</sub> UK) Crysfire program<sup>20</sup> which provided information about the crystal system of OMFs. Efforts to prepare single crystals of OMFs were unsuccessful due to high molecular mass of metal ions. Hence, powder X-ray diffraction pattern analysis of OMFs was specially discussed. The diffraction pattern revealed the crystalline nature of OMFs for concerned crystal system. GSAS program for space group and density were determined by the Archimedes method. Mixed ligands formed OMFs which were derived from Bi(V) due to vacant 6d-orbital of this metal, accepted electron from N/O.

#### MOLECULAR MODELLING OF OMFs

Molecular modelling helped to demonstrate the significant features i.e. molecular geometries, bond energies, torsion angles and Cartesian coordinates of OMFs theoretically. Bond lengths, bond angles and atomic coordinates depend on the hybridization of an atom and mode of bonding. Thus, molecular modelling was the blueprint of three dimensional arrangements of atoms. Beside this, if deviations in bond distances, bond angles or torsion angles were evidenced, specific electronic interactions can be detected and confirmed the earlier spectral evidences.<sup>21</sup> The bonding capabilities of atoms/metal ions have impact on bond lengths and bond angles of concerned functional groups. Therefore, molecular models of OMFs were demonstrated. Physical dimension of the molecules helped out to demonstrate the changes occurred during their topological assemblies. Energy minimization did numerous

**Table 3.** Crystallographic data of OMFs

Compounds	(L <sub>1</sub> )	(L <sub>2</sub> )
Formula	C <sub>44</sub> H <sub>61</sub> BiN <sub>8</sub> O <sub>20</sub>	C <sub>32</sub> H <sub>36</sub> BiN <sub>6</sub> O <sub>21</sub> S <sub>2</sub> Cl <sub>3</sub>
FW	1230.970	1220.13
Temp (K)	293	293
Wavelength	1.54056	1.54056
Crystal System	Triclinic	Monoclinic
Space group	P1	P 2/m
Unit cell dimension		
a(Å)	8.983043	12.31927
b(Å)	8.983043	13.25236
c(Å)	12.09464	7.98259
α(°)	112.256	90.000
β(°)	96.153	106.23
γ(°)	69.548	90.000
Volume (Å <sup>3</sup> )	178.293	913.26
θ range (°)	12-75.00	9-80
Limiting indices	-3 ≤ h ≤ 1 -4 ≤ k ≤ 4 0 ≤ l ≤ 4	-7 ≤ h ≤ 5 0 ≤ k ≤ 8 0 ≤ l ≤ 5
R indices	0.0000713	0.0000505
Density g/(cc)	1.146	1.791
Z	2	1

times to elaborate global minimum energy<sup>22,23</sup> Data analysis of bond lengths and angles were presented in table 2 to 5. Following remarks were concluded:

By molecular models analysis, it was observed that in Bi(V)OMC-1, Bi(V) has distorted-bipyramidal environment, defined by four O atoms and one N atom at the equatorial site and the axial site respectively, table 4 and 5. Bonds angles between Bi(V) and O/N for OMF-1 were altered between O(71)-Bi(37)-N(12) and N(12)-Bi(37)-O(10) found 119.9° and 104.0° respectively. OH and -NH- groups took part in bond formation with Bi(V) in OMFs via -O-Bi and C-N-Bi- linkages. Coordination significantly shortened as 2.136 [Å] for N(12)-Bi(37) as compared to 2.1 [Å] for O(71)-Bi(37). This was because of bond lengths of hydroxyl (OH), carbonyl (>C=O) and secondary amine (-NH-) groups probably got affected due to the formation of bonds with Bi(V). There was a large variation in O(39)-Bi(37) bond lengths on framework and becomes slightly longer as the coordination took place via N atom of -N-CH<sub>3</sub>.

By molecular models revealed that Bi(V)OMC-2, has a distorted-bipyramidal environment in which Bi(V) surrounded by two O atoms and three OClO<sub>3</sub> atoms at the equatorial site and at the axial site respectively, table 6 and



7. Bonds angles between Bi(V) and -O- for OMF-2 were altered between O(56)-Bi(50)-O(51) and Bi(50)-O(48)-O(24) and found as 180.0° and 120.0° respectively. Carbonyl groups (>C=O) took part in bond formation via -O-Bilinkages. Coordination significantly shortened from 2.100 [Å] for O(24)-Bi(50) as compared to 2.11 [Å] for Bi(50)-P(61). This was because of bond lengths of >C=O probably influenced due to new bond formation with Bi(V). There was a large variation in O(24)-Bi(50) bond lengths on framework which became slightly longer as the coordination took place via -O- atom of >C=O.

Based on spectral and analytical analysis (elemental analysis, conductance measurement, infrared, <sup>1</sup>H and <sup>13</sup>C NMR, electronic, mass, molecular modelling) and solvent accessible surface models of Bi-OMFs were designed and presented in figure 2 to 5.

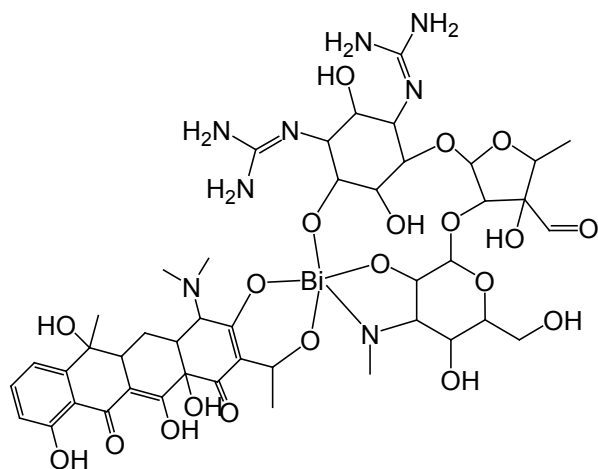


**Figure 2.** Molecular structure of OMF-1

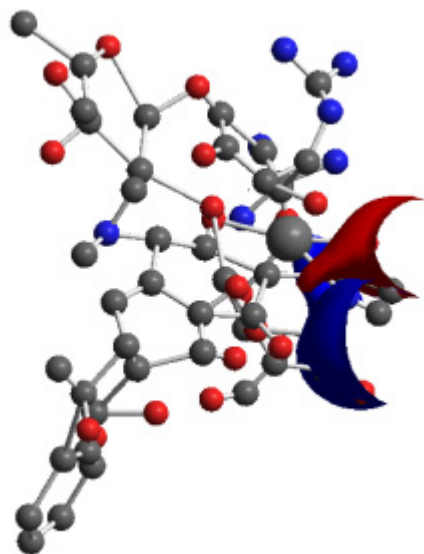


**Figure 3.** Molecular model of OMF-1 with LOMO : Color Code, Red, Oxygen; Blue, Nitrogen; Grey, Carbon

**Table 4.** Bond Lengths of OMF-1

Sr. No.	Geometrical sequencing of atoms	Bond Length (°)
1	O(69)-Bi(37)	2.1100
2	O(71)-Bi(37)	2.1020
3	O(32)-Bi(37)	2.1000
4	O(10)-Bi(37)	2.1030
5	N(12)-Bi(37)	2.1360

**Table 5.** Bond Angles of OMF-1

Sr. No.	Geometrical sequencing of atoms	Bond Length (°)
1	C(68)-O(71)-Bi(37)	126.1676
2	C(57)-O(69)-Bi(37)	109.5000
3	O(71)-Bi(37)-N(12)	119.9994
4	O(71)-Bi(37)-O(10)	119.9994
5	O(69)-Bi(37)-O(32)	133.5194
6	O(69)-Bi(37)-N(12)	119.9988
7	O(69)-Bi(37)-O(10)	120.0000
8	N(12)-Bi(37)-O(10)	104.0000
9	Bi(37)-O(32)-C(27)	109.5000
10	Bi(37)-O(10)-C(5)	104.0000

Atomic coordinates parameters of OMF-1

Atom	x	y	z
1) O	4.3252	4.7620	-2.3617
2) C	5.5707	4.6202	-1.4000
3) C	4.6123	3.8645	-0.4889
4) C	4.4637	2.4322	-0.9846
5) C	3.9054	2.4400	-2.4016
6) C	4.4798	3.6248	-3.1670
7) C	6.1048	5.9296	-0.8347
8) O	7.4968	5.9757	-0.9957
9) O	5.1196	3.8559	0.8181
10) O	4.4265	1.2731	-2.9780
11) O	5.8764	3.5030	-3.1464
12) N	5.0026	1.2853	0.3100
13) O	6.2017	0.1794	-4.2927
14) C	7.9518	0.8805	-4.4656
15) C	7.7215	2.3182	-4.0188
16) C	6.2063	2.4713	-4.0365
17) C	5.6972	1.1677	-3.4357
18) C	8.4443	0.8121	-5.9051
19) C	8.2663	2.5412	-2.6294
20) O	9.0951	3.3985	-2.4360
21) O	8.3678	3.2498	-4.8434

22) O	6.4606	0.9053	2.2894
23) C	6.5894	2.6605	1.0556
24) C	6.9533	1.6491	-0.1046
25) C	6.2918	2.0006	-1.4307
26) C	4.7956	2.1890	-1.2174
27) C	5.7488	3.4206	-1.1582
28) C	5.9678	3.8238	0.2940
29) O	6.5365	0.3656	0.2754
30) O	7.7366	3.0664	1.7519
31) N	6.8700	4.9830	0.3494
32) O	6.7037	2.4435	-1.4731
33) N	3.8681	2.0327	-2.3470
34) C	6.4762	6.0672	0.8712
35) N	7.2496	7.0609	0.9187
36) N	5.3055	6.1530	1.3452
37) Bi	5.7812	0.5582	-1.5414
38) C	2.7210	1.5309	-2.1595
39) N	1.9260	1.3969	-3.1278
40) N	2.3728	1.1636	-0.9991
41) C	10.1681	-8.1965	5.5483
42) C	11.6563	-7.9910	3.9038
43) C	11.5398	-6.6591	3.9038
44) C	10.3281	-6.0940	3.9038
45) C	9.2328	-6.8609	3.9038
46) C	9.1529	-7.9121	4.7260
47) C	10.1541	-4.7543	3.8921
48) C	9.2968	-4.2981	2.9529
49) C	8.4813	-5.2642	2.1512
50) C	8.1673	-6.4896	2.9994
51) C	9.2073	-2.9789	2.7548
52) C	8.2783	-2.4052	1.7307
53) C	7.7741	-3.5188	0.8222
54) C	7.1966	-4.6439	1.6708
55) C	9.0253	-1.4132	0.8734
56) C	8.3714	-1.0138	-0.2393
57) C	7.2655	-1.6827	-0.5815
58) C	6.7657	-2.8333	0.2353
59) O	12.6497	-5.8819	3.9038
60) O	10.7226	-4.0192	4.6639
61) O	9.9739	-2.1435	3.4966

62) O	10.1260	-1.0066	1.1606
63) C	7.8990	-7.6631	2.0664
64) O	7.0547	-6.1664	3.7889
65) N	5.8917	-2.3285	1.2596
66) C	4.7982	-1.6211	0.6500
67) C	5.3803	-3.4257	2.0359
68) C	8.8786	0.1284	-1.0634
69) O	6.5130	-1.4057	-1.6738
70) O	7.2075	-1.7816	2.3864
71) O	7.8463	0.6363	-1.9150
72) C	9.3535	1.2401	-0.1371
73) C	3.9943	0.4970	0.9655

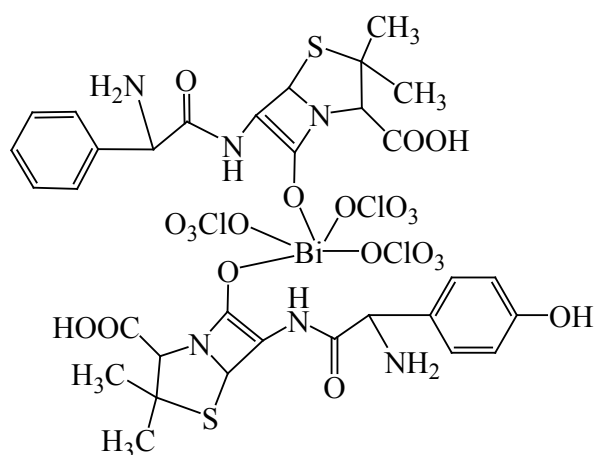


**Figure 4.** Molecular structure of OMF-2

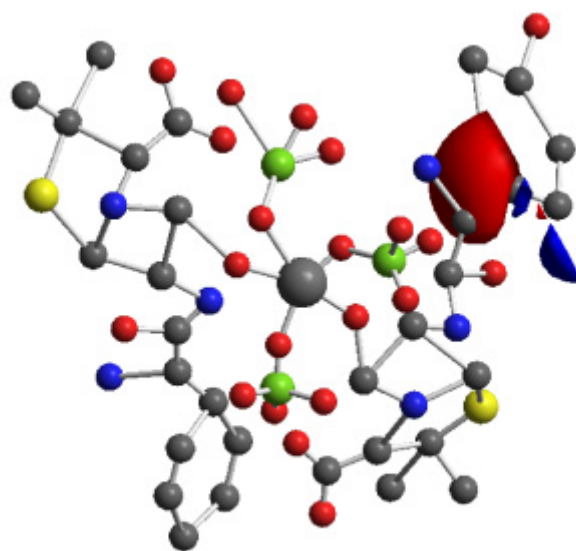


**Figure 5.** Molecular model of OMF-2 with LOMO: Color Code, Red, Oxygen; Blue, Nitrogen; Grey, Carbon

**Table 6.** Bond Lengths of OMF-2

Sr. No.	Geometrical sequencing of atoms	Bond Length (°)
1	Bi(50)-O(61)	2.1050
2	Bi(50)-O(56)	2.1010
3	Bi(50)-O(51)	2.1060
4	O(24)-Bi(50)	2.1040
5	O(48)-Bi(50)	2.1020

**Table 7.** Bond Angles of OMF-2

Sr. No.	Geometrical sequencing of atoms	Bond Length (°)
1	Cl(62)-O(61)-Bi(50)	120.1000
2	Cl(57)-O(56)-Bi(50)	120.2000
3	Cl(52)-O(51)-Bi(50)	120.1200
4	O(56)-Bi(50)-O(51)	180.0030
5	O(48)-Bi(50)-O(24)	180.1000
6	Bi(50)-O(48)-C(35)	120.0400

## Atomic coordinates parameters of OMF-1

Atom	x	y	z
1) C	1.7531	7.7298	-3.8105
2) C	1.5058	8.2612	-2.6089
3) C	1.8164	7.5813	-1.5004
4) C	2.3744	6.3698	-1.5936
5) C	2.6217	5.8384	-2.7952
6) C	2.3111	6.5183	-3.9037
7) C	2.7223	5.6085	-0.3524
8) N	2.0026	4.3637	-0.3370
9) C	4.2057	5.3330	-0.3314
10) C	5.8722	3.9085	-0.2870
11) C	6.8076	2.7511	-0.2555
12) C	7.1686	4.6570	-0.2870
13) N	7.9036	3.3839	-0.2870
14) S	7.4296	5.3147	1.3844
15) C	7.8865	3.7343	2.1512
16) C	8.5883	3.1709	0.9962
17) C	8.8004	3.9149	3.3560
18) C	6.7485	2.9032	2.7289
19) C	8.7367	1.6848	1.2120
20) O	9.8372	1.1930	1.2920
21) O	7.6494	0.9118	1.3147
22) O	4.9908	6.2511	-0.3400
23) N	4.6276	4.1396	-0.3047
24) O	6.5603	1.4198	-0.2074
25) C	14.6555	-7.6743	-3.5103
26) C	14.8697	-8.1863	-2.2940
27) C	14.5290	-7.4887	-1.2055
28) C	13.9741	-6.2791	-1.3333
29) C	13.7598	-5.7670	-2.5497
30) C	14.1005	-6.4646	-3.6382
31) C	13.5926	-5.4980	-0.1146
32) N	14.3119	-4.2529	-0.0995
33) C	12.1091	-5.2225	-0.1385
34) C	10.4424	-3.7978	-0.1626
35) C	9.5068	-2.6403	-0.1753

36) C	9.1463	-4.5465	-0.1861
37) N	8.4118	-3.2738	-0.2266
38) S	8.8396	-5.1773	1.4879
39) C	8.3622	-3.5850	2.2165
40) C	7.6924	-3.0403	1.0339
41) C	7.4157	-3.7464	3.3986
42) C	9.4842	-2.7444	2.8117
43) C	7.5385	-1.5510	1.2216
44) O	6.4363	-1.0582	1.2636
45) O	8.6227	-0.7762	1.3416
46) O	11.3244	-6.1408	-0.1539
47) N	11.6870	-4.0290	-0.1425
48) O	9.7530	-1.3083	-0.1419
49) O	15.0008	-8.3813	-4.6135
50) Bi	8.1566	0.0557	-0.1746
51) O	8.1753	0.1280	1.9240
52) Cl	7.1094	1.0730	2.7165
53) O	5.8038	0.6699	2.4035
54) O	7.3164	0.9529	4.0977
55) O	7.2914	2.4081	2.3299
56) O	8.1380	-0.0165	-2.2733
57) Cl	7.0576	0.8723	-3.1098
58) O	5.7580	0.4925	-2.7468
59) O	7.2401	0.6574	-4.4830
60) O	7.2456	2.2307	-2.8193
61) O	6.7923	-1.5393	-0.1076
62) Cl	5.1898	-1.2414	-0.1036
63) O	4.8401	-0.5462	-1.2695
64) O	4.4897	-2.4550	-0.0564
65) O	4.8614	-0.4674	1.0180

**ANTIFUNGAL EFFECTIVENESS OF OMFs**

Metal frameworks played a vital role in different biological processes. The interaction of microbial agents with biologically active OMFs was of great interest. Designing and tailoring of new biologically active OMFs were crucial which depended on the utilization of new methodologies and implemented techniques significantly. These biologically active compounds acted because of metal and donor atoms interactions. OMFs and mixed ligands were tested and reported against different fungal strains i.e. *Candida albicans*, *Aspergillus flavis* and *Candida glaberata*. The screening results presented graphically in figure 6. Antimicrobial effectiveness of OMFs depended upon several factors i.e. metal ion(s), chromophore set of ligands and geometrical features. The combined impact of these factors made OMF moiety competent as needed. OMFs having tailored architectures and appropriate metal/ligand stability within the approach of ligands moieties as per the needs of a good antifungal agent. Moreover, coordination reduced the polarity of metal ion(s) because of partial sharing of its positive charge with different functional groups of the ligands having  $\pi$ -electron delocalization. During this process, lipophilic nature of central metal atom increased as a result, it favoured permeation more efficiently through the lipid layer of the microorganism to destroy them more aggressively. Besides this, probably there might be other factors such as solubility, dipole moment and conductivity which influenced by metal ion(s). OMFs showed higher activity than free ligand because of increased activity of

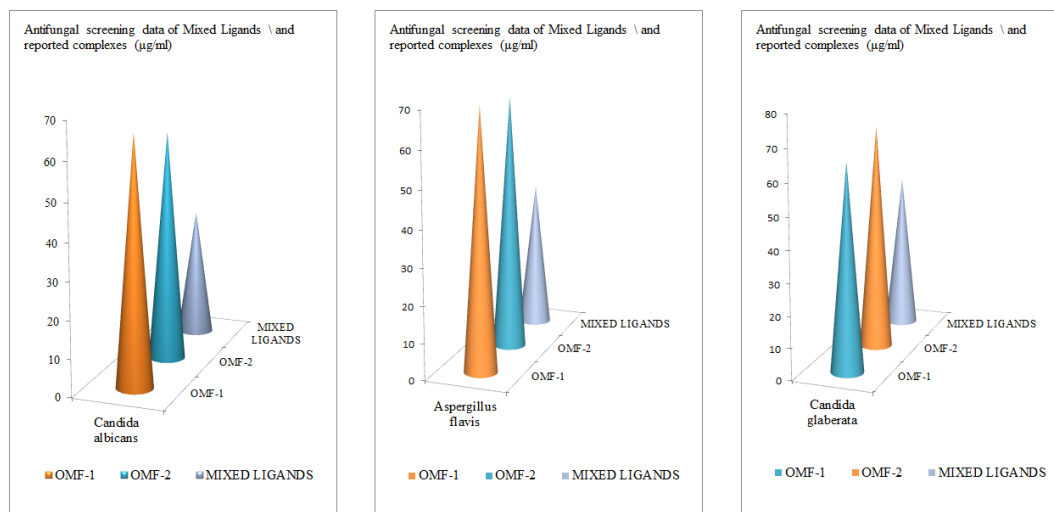


**Figure 6.** Antifungal activities of OMFs

metal chelates.<sup>24</sup> These could be the major reasons behind the higher antimicrobial effectiveness of OMFs than mixed ligands.<sup>25</sup>

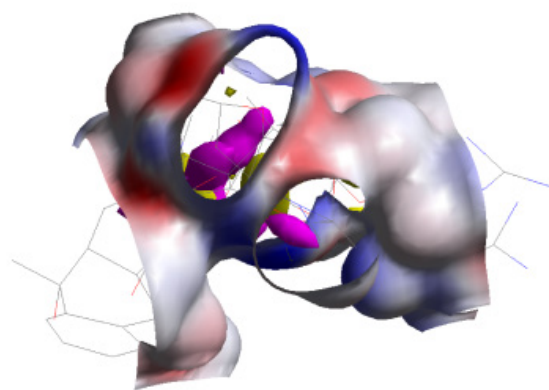


**Figure 7.** Pharmacophore geometry for OMF-1



**Figure 8.** Pharmacophore geometry for OMF-2

OMFs were directly mixed in a medium of different concentrations. Antifungal activity of mixed ligands and

OMFs were performed by agar plate technique against *Candida albicans*, *Aspergillus flavus* and *Candida glabrata* and screened values were presented. Reported OMFs have potential to generate novel antimicrobial agent by displaying moderate to high affinities for most of the receptors particularly in case of OMFs-1.

Cell permeability was due to its surrounding by lipid membrane and acted as a special passage for lipid soluble materials. So, it showed liposolubility and increased antimicrobial resistance in a cell. This was known as the most important biological phenomenon in regard to antifungal aspects. Keeping in view the problem of antimicrobial resistance, reported OMFs showed good antimicrobial effectiveness. The inhibition activity of compounds seems to govern with certain degree as per the availability percentile of nitrogen atoms in ligands and OMFs. This was why OMFs-1 showed more activity against *Candida albicans* compared to OMF-2 which has lesser nitrogen atoms. Presented results showed that OMFs were more active than mixed ligands. The activity probably increased due to variation in structure after complexation and the presence of different ring system in its moiety.

## CONCLUSION

Elemental analysis showed monomeric nature of OMFs. For a better insight into the nature of these architectures, molecular models were achieved by using theoretical and topological analysis, i.e. using multidimensional approach through molecular models and spectral investigations. Network of tactics at molecular level were discussed to understand three dimensional atomic arrangements of OMFs. Adjustability / connectivity / selection abilities of ligand towards Bi(V) through its specific coordination sites were explored. Spectral results proved Bi(V) was coordinated through -O- of hydroxyl and carbonyl groups of neighbouring rings. In the architecture and tailoring of such multidimensional networks, antibiotics as organic moieties having bonding sites which were used for the formulation of OMFs.<sup>26</sup> These coordination modes and intriguing architectures have the possibility of rationally designing and synthesizing supramolecular architectures based on covalent



bonded formation between oxygen/nitrogen atoms of ligands and Bi(V) as reported earlier.<sup>27</sup> Vibrational spectral analysis, UV, <sup>1</sup>H-NMR, <sup>13</sup>C-NMR spectra of MOFs confirmed the same bonding setup by showing disappearance of some hydroxyl groups protons especially from the substituent groups of tetrahydrofuran and neighbouring cyclic rings. Cell parameters and molecular modeling had been done to find out optimization energies to get refined models in three dimensions of OMFs.

Metal centre was capable of organizing surrounding atoms to achieve pharmacophore geometries that were not rapidly and readily achieved by other means, figure 7 and 8. Additionally, the effect of metals can be highly specific and modulated by recruiting cellular processes that recognize specific types of metal macromolecule interactions. To understand these specific interactions which led the way towards rational design of metallopharmaceuticals and implementation of new co-therapies, such interaction has a great importance to be addressed. Metals might be useful in active site recognition and in bifunctional agents<sup>28</sup> as secondary contacts to increase inhibitor affinity. OMFs can be potent and highly selective ligands of cell surface receptors and shown potent antimicrobial activities in a variety of screens.

Although it was difficult to make out an exact structure which can directly use to explain the activity relationship between antimicrobial species and topologies of OMF. It can possibly be concluded that the biological activity of the ligands exhibited a marked enhancement on coordination with bismuth ions against all tested fungal strains which showed that bismuth(V) chelates were more active than the ligands.<sup>29,30</sup> On chelation, polarity of the metal ion was reduced to a greater extent due the overlapping of the ligand orbitals and partial sharing of the positive charge of Bi(V) with bonded electronegative atoms. Moreover, delocalization of p-electrons over the whole chelate ring was increased and lipophilicity of OMFs was enhanced. The increased lipophilicity enhanced penetration of OMFs into lipid membranes and blocks Bi(V) sites in enzymes of microbial.

## EXPERIMENTAL

### MATERIALS AND INSTRUMENTS

All the chemicals and solvent used in this study were of Analytical Reagent grade and used as procured from Aldrich and dried over 4 Å molecular sieves. Solvents were purified by standard procedures.<sup>31</sup> The elemental analysis (C, H and N) of OMFs were performed using a Carlo-Ebra 1106 elemental analyzer. Mass spectra were recorded on a MAT 8500 Finnigan (Germany). Metal content was estimated on AA-640-13 Shimadzu flame atomic absorption spectrometer in solution prepared by decomposing the respective frameworks in hot concentrated HNO<sub>3</sub>. IR spectra were recorded on a Perkin-Elmer FTIR spectrometer in KBr. The electronic spectra were recorded in water on a Beckman DU-64 spectrometer with quartz cells. <sup>1</sup>H and <sup>13</sup>C NMR spectra were recorded at ambient temperatures on Bruker AMX400 and DRX500 spectrometers with TMS as internal reference

and D<sub>2</sub>O as solvent. Chemical shifts (δ) were expressed in parts per million (ppm) relative to (TMS) tetramethylsilane.

### XRPD Analysis

Various attempts to obtain single crystals remained unsuccessful. X-ray powder diffraction studies indicated the crystalline nature of the OMFs. All the compounds were soluble in polar solvents. The crystals needed for X-ray powder diffraction analysis were tried to produce crystalline forms as follows: one gm of Bi-OMF was dissolved at 40 °C in minimum amount of methanol. A clear solution was obtained and heated for 4 to 5 minutes under reflux and was then filtered off at a high temperature. The solution was cooled down to room temperature and closed with a semipermeable membrane so that methanol cannot evaporate but still a very slow evaporation was there. The mixtures were stored at room temperature for a period of three to five weeks. Very small crystals were filtered off and dried.

XRPD patterns were recorded on a vertical-type Philips 1130/00 X-ray diffractometer, operated at 40 kV and 50 mA generator using Cu-Kα line at 1.54056 Å as the radiation sources. Sample was scanned between 5° to 70° (2θ) at 25 °C. Crystallographic data was analyzed using CRYSFIRE-2000 powder indexing software package and the space group was found by CHECK CELL programme. Debye-Scherrer relation was derived with the help of 100% peak width to determine the particle size. Experimental density was observed through Archimedes method.

### 3D Molecular Modeling

Correct sequence of atoms was obtained to get reasonable low energy molecular models to determine their molecular representation in three dimensions. Complications of molecular transformations could be explored using output obtained. An attempt to gain a better insight on molecular structure of OMCs, geometric optimization and conformational analysis were performed using MM+2 force field.<sup>32</sup> Potential energy of molecule was the sum of following terms: E = Estr + Eang + Etor + Evdw + Eoop + Eele. where all E's represent energy values and found corresponds to given types of interaction. The subscripts str, ang, tor, vdw, oop and ele denote bond stretching, angular bonding, torsion deformation, van der waals interactions, out of plane bending and electronic interaction, respectively.

### Pharmacology: In-vitro Antifungal Assay

Antifungal activities of ligands and OMF-1 to OMF-2 were screened against *Candida albicans*, *Aspergillus flavis* and *Candida glaberata* by preparing their stock solutions in DMSO according to required concentrations for experiments. To ensure the effect of solvent on bacterial growth, a control test was performed with test medium supplemented with DMSO. Growth of fungus was measured by reading diameter of fungal colony. Screening for antifungal activities was carried out in vitro<sup>33</sup> and relative inhibitory ratios (%) were determined using mycelium growth rate method. On complete mycelia growth, its diameters were measured and inhibition rate was calculated

according to formula:  $I = \frac{(\overline{D}_t - \overline{D}_o)}{\overline{D}_t} \times 100$  where I is inhibition rate,

$D_1$  is average diameter of mycelia in the blank test and  $D_0$  being average diameter of mycelia in presence of OMFs.

### Preparation of Metal Solution

Corresponding metal salts were dissolved in mixture of ethanol and 0.1 M HCl and then filtered. The transparent filtrate was obtained as metal salt and further used for frame workstation.

### Preparation of M-APT Solution

M-APT solution was prepared by drop-wise addition of metal salts solution to 100 ml of 0.01 M APT solution in methanol with continuous stirring at room temperature. The pH of the solution was adjusted by drop-wise addition of NaOH in the range of 2-3 using a pH-meter separately.

### Synthesis of OMF-1

OMF-1 of Bi(V) was prepared by dissolving equimolar amounts of 5-(2,4-diguanidino-3,5,6-trihydroxy-cyclohexoxy)-4-[4,5-dihydroxy-6(hydroxymethyl)-3-methylamin-tetrahydropyran-2-yl]oxy-3-hydroxy-2-methyltetrahydrofuran-3-carbaldehyde (0.2905 g, 0.5 mmol) and 2-(amino-hydroxymethylidene)-4-dimethylamino-6,10,11,12-tetrahydroxy-6-methyl-4,4a,5,5a-tetrahydro-tetracene-1,3,12-trione (0.120 g, 0.5 mmol) and Bi(V) (0.068 g, 0.5 mmol) in minimum quantity of  $\text{CH}_3\text{OH}$  (25 mL, absolute) and bi-distilled (carbon dioxide free) water in a 100 mL round bottom flask. The mixture was heated for 6 h at  $\sim 82^\circ\text{C}$  on a water bath to reduce the volume of the solution to  $\sim 12$  mL. A solid mass was separated out on cooling at  $\sim 5^\circ\text{C}$  and kept in a refrigerator for better crystallization. It was then filtered, washed with  $\text{CH}_3\text{OH}$ , and dried over  $\text{P}_2\text{O}_5$  under vacuum. The crystals were re-dissolved for recrystallization with warm methanol, resulting in a clear solution which when left undisturbed for weeks formed very small crystals.

### Synthesis of OMF-2

OMF-2 of Bi(V) was prepared by dissolving equimolar amounts of (6R)-6-( $\alpha$ -phenyl-D-glycylamino) penicillanic acid (0.1827 g, 0.5 mmol); hydroxyl derivative of (6R)-6-( $\alpha$ -phenyl-D-glycylamino) penicillanic acid (0.1889 g, 0.5 mmol) and Bi(V) (0.068 g, 0.5 mmol) in minimum quantity of  $\text{CH}_3\text{OH}$  (25 mL, absolute) and bi-distilled (carbon dioxide free) water in a 100 mL round bottom flask. The mixture was heated for 6 h at  $\sim 85^\circ\text{C}$  on a water bath to reduce the volume of the solution to  $\sim 12$  mL. A solid mass was separated out on cooling at  $\sim 5^\circ\text{C}$  and kept in a refrigerator for better crystallization. It was then filtered, washed with  $\text{CH}_3\text{OH}$ , and dried over  $\text{P}_2\text{O}_5$  under vacuum. The crystals were re-dissolved for recrystallization with warm methanol, resulting in a clear solution which when left undisturbed for weeks formed very small crystals.

Almost all of the Bi(V) complexes were very unstable in aqueous media. Their stability in aqueous media was attributed to the steric shielding of Bi(V) in the compound. Stable Bi(V) OMCs also required strong electronegative bonding partners. Stability studies of OMCs exploiting its VIS absorption spectrum indicated that it slightly undergo decomposition in aqueous medium, a fact that can attributed to the oxidants and electrophiles properties of the five and six

membered cyclic systems<sup>34</sup> as earlier reported by the author.<sup>35-37</sup>

### ACKNOWLEDGEMENTS

Authors acknowledge I.I.T. Bombay for recording EPR and  $^1\text{H}$ -NMR spectra and IIT Madras, India for recording magnetic moments.

### REFERENCES

1. Mohan, R. Green bismuth. *Nature Chem.* **2010**, *2*, 336-336.
2. Sun, H. Z.; Zhang, L.; Szeto, K. Y. Bismuth in medicine, in metal ions in biological systems, metal ions and their frameworks in medication. Marcel Dekker, 270, Madison Ave, New York, NY 10016 USA, **2004**, *41*, 333-378.
3. Graham, D. Y.; Fischbach, L. Helicobacter pylori treatment in the era of increasing antibiotic resistance. *Gut.* **2010**, *59*, 1143-1153.
4. Diaz-Bone, R. A.; Van, de W. T. Biotransformation of metal(loid) s by intestinal microorganisms. *Pure Appl. Chem.* **2010**, *82*, 409-427.
5. Kadhum, A. A. H.; Mohamad, A. B.; Al-Amiery, A. A.; Takriff, M. S. Antimicrobial and antioxidant activities of new metal frameworks derived from 3-aminocoumarin. *Molecules*, **2011**, *16*, 6969-6984.
6. Kheira, F.; Abdelkarim, B.; Abdelkader, C.; Abdellah, M.; Gérard, B.; Douniazed, E. A. Synthesis and structural study of triphenylbismuth bis(salicylate). *Crystal struct. theory and appl.* **2013**, *2*, 28-33.
7. Frank, T.; Beatrix, B.; Reinhard, H. Medical use of bismuth: the two sides of the coin, S3:004. doi:10.4172/2161-0495.
8. Singh, J. Effect of heavy metals and sewage on seed germination and plant growth. *Int. Arch. Sci. Technol.*, **2006**, *6*(1), 1-4.
9. Azza, A. A.; Abu-Hussen, Wolfgang, L. Redox, thermodynamic and spectroscopic of some transition metal frameworks containing heterocyclic Schiff base ligands. *Spectrochimica Acta Part A*, **2009**, *74*, 214-223.
10. Eng, G.; Whalen, D.; Musingarimi, P.; Tierney, J.; DeRosa, M. Fungicidal and spectral studies of some triphenyltin compounds. *Appl. Organomet. Chem.*, **1998**, *12*, 25-30.
11. Joshi, A.; Verma, S.; Jain, A.; Saxena, S. Synthetic pathway, structural chemistry and structural elucidation based upon spectral studies [IR, NMR ( $^1\text{H}$ ,  $^{13}\text{C}$  and  $^{119}\text{Sn}$ )] of some mixed ligand frameworks of diorganotin(IV) derived from satirically demanding heterocyclic  $\beta$ -diketones and N-protected amino acids. *Main Group Metal Chem.*, **2011**, *7*, 123-134.
12. Singh, H. L.; Singh, J. B.; Sharma, K. P. Synthetic, structural, and antimicrobial studies of organotin(IV) frameworks of semicarbazone, thiosemicarbazone derived from 4-hydroxy-3-methoxybenzaldehyde. *Research on Chem. Intermediates*, **2012**, *38*, 53-65.
13. Deacon, G. B.; Phillips, R. J. Relationships between the carbon-oxygen stretching frequencies of carboxylato frameworks and the type of carboxylate coordination. *Coord. Chem. Reviews*, **1980**, *33*, 227-250.
14. Ferraro, J. R.; Low Frequency Vibrations of Inorganic and Coordination Compounds, Plenum Press: New York, 1971. David, M. A.; Metal-Ligand and Related Vibrations. Edward Arnold: London, 1967.
15. Bellamy, C. J.; Infrared Spectra of Frameworks Molecules, Methuen: London, 1959.
16. Otwinowski, Z.; Minor, W.; Processing of X-ray Diffraction Data Collected in Oscillation Mode. Macromolecular Crystallography. Academic Press: San Diego, CA, 1997.
17. Kheiri, F. M.-N.; Tsipis, C. A.; Manoussakis, G. E. Syntheses and spectroscopic study of some new mixed-ligand Bi(III) 1,1-dithiolate frameworks. *Inorg. Chim. Acta*, **1997**, *25*, 223-227.
18. Manoussakis, G. E.; Tsipis, C. A.; Hadjikostas, C. C. Five-coordinate bromobis(dialkylthiocarbamate) frameworks of arsenic, antimony, and bismuth. *Canad. J. of Chem.*, **1975**, *53*, 1530-1535.
19. Ram, M. S.; Hupp, J. T. Generalized synthesis of cis- and trans-dioxorhenium(V) (bi)pyridyl frameworks. *Inorg. Chem.*, **1991**, *30*, 130-133.
20. Shirly, R. The CRYSFIRE System for Automatic powder Indexing: User's Manual, Lattice Press: Guildford, UK, 2002.
21. Comba, P.; Hambley, T. W. Molecular Modeling of Inorganic Compounds, VCH, Weinheim, 1995.

22. Murthy, A.P. Electrochemical reductive cleavage of carbon-halogen bonds – application of Marcus theory in the analysis of nonlinear activation-driving force relationships. *Int. Arch. Sci. Technol.*, **2006**, 6(1), 10-15.
23. Kumar, R.; Mishra, P.; Singh, R. P.; Singh, R. P. Synthesis, spectroscopic, XRPD and computational study of transition metal-organic frameworks (TMOFs) derived from (6R)-6-( $\alpha$ -Phenyl-D-Glycylamino) penicillanic acid. *Russ. J. of Inorg. Chem.*, **2009**, 54, 1301-1309.
24. Abdallah, S. M.; Mohamed, G. G.; Zayed, M.A.; Abou, El-Ela, M. S. Spectroscopic study of molecular structures of novel Schiff base derived from o-phthaldehyde and 2-aminophenol and its coordination compounds together with their biological activity, *Spectrochim Acta A*, **2009**, 1, 833-40.
25. Chohan, Z. H.; Scozzafava, A.; Supuran, C. T. Zinc frameworks of benzothiazole-derived Schiff bases with antibacterial activity. *J. of Enzy. Inhib. and Med. Chem.*, **2003**, 18, 259-263.
26. Arish, D.; Nair, M. N. Synthesis, characterization and biological studies of Co(II), Ni(II), Cu(II) and Zn(II) frameworks with pyrrol-histidinate. *Arab. J. of Chem.*, **2012**, 5, 179-186.
27. Rajiv, K.; Rajni, J. Computational approach on architecture and tailoring of organic metal frameworks derived from streptomycin and Zn, Cd and Pb: antimicrobial effectiveness, *Appl. Organometal. Chem.*, **2011**, 25, 791-798.
28. Chhikara, B.S., Mishra, A.K., Tandon, V. Synthesis of Bifunctional Chelating Agents to label monoclonal antibodies for radioimmunodiagnosis of cancer. *Int. Arch. Sci. Technol.*, **2006**, 6(1), 5-9.
29. Seely, H. W.; Van, Demark, P. J. *Microbes in Action, Laboratory of Microbiology*, 3<sup>rd</sup> Edition. W. H. Freeman and Co. USA, 1981.
30. Zuo, J.; Bi, C.; Fan, Y. Cellular and computational studies of proteasome inhibition and apoptosis induction in human cancer cells by amino acid Schiff base-copper frameworks. *J. of Inorg. Biochem.*, **2013**, 118, 83-93.
31. Riddick, J. A.; Bunger, W. B.; *Organic Solvents: Physical Properties and Methods of Purification*, 3<sup>rd</sup> Edition, Wiley-interscience: New York, 1970.
32. Allinger, N. L.; *Molecular Structure: Understanding Steric and Electronic Effects from Molecular Mechanics*, John Wiley & Sons, 2010.
33. Collins, C. H.; Lyre, P. M.; Grange, J. M.; *Microbiological methods*, 6<sup>th</sup> Edition, Butterworth: London, 1989.
34. Busev, A. I.; Tiptsova, V. G.; Ivanov, M. V. *Analytical Chemistry of Rare Elements*, Moscow, Russian Edn., 1981.
35. Rajiv, K.; Mishra, P. Spectroscopic, thermal, X-ray powder diffraction parameters of Bi(V) complexes with [2S-[2fN, 5fN, 6fO(S)]-6-amino(4 hydroxyphenyl) acetyl amino]-3,3-dimethyl-7-oxo-4-thia-1-azabicyclo[3,2,0] heptane-2-carboxylic acid and (6R)-6-(fN-phenyl-D-glycylamino) Penicillinic Acids. *Main Group Chem.* **2008**, 7, 1-14.
36. Rajiv, K.; Mishra, P. Bi(V) Organic framework in an asymmetric system: synthesis, spectroscopic, XRPD and molecular modeling. *Main Group Chem.* **2007**, 6, 85-95.
37. Rajiv, K.; Mishra, P. Metal-organic frameworks of Bi and Pb Derived from 2-[4,6-diamino-3-[3-amino-6-(1-methylamino-ethyl) tetrahydropyran-2-yl] oxy-2-hydroxycyclohexoxy]-5-methyl-4-methylamino-tetra hydropyran-3,5-diol and its Molecular modelling. *Main Group Chem.* **2007**, 6, 1-14.